EFFECTS OF DISSOLUTION CONDITIONS ON THE RECOVERY OF SAMARIUM PHOSPHATE FROM PRACTICAL MAGNETS

Hiroaki Onoda[a]*, Atsuya Iinuma[b]

Abstract: Samarium-cobalt alloys are used as materials for powerful magnets with relatively high Curie temperatures. Samarium is one of the rare earth elements and is a valuable and expensive element. Recovery, reuse, and recycling of rare earth elements are necessary to protect this rare earth resource. Recently, a new two-step precipitation method to recover samarium phosphate from transition metal mixtures has been reported. Since rare earth phosphates are the main component of rare earth ores, a new method has been proposed to recover rare earth elements as phosphates. In this study, we attempted to obtain samarium phosphate by this two-step precipitation method by dissolving the actual magnet used. This method can separate and recover samarium phosphate from mixed metal ion aqueous solutions without the use of high temperatures or special equipment. In this study, nitric acid, hydrochloric acid, and sulfuric acid were examined as acids that dissolve the magnet. The dissolution of magnets with acid in amounts equal to, double, and triple the chemical equivalent was investigated.

Keywords: rare earth recovery; phosphoric acid; precipitation

[a].   Department of Informatics and Environmental Sciences, Kyoto Prefectural University, 1-5, Shimogamo Nakaragi-cyo, Sakyo-ku, Kyoto 606-8522, Japan

[b].   Department of Informatics and Environmental Sciences, Kyoto Prefectural University, 1-5, Shimogamo Nakaragi-cyo, Sakyo-ku, Kyoto 606-8522, Japan

*Corresponding Author

E-mail: h-onoda@kpu.ac.jp

INTRODUCTION

Samarium-cobalt permanent magnets have high magnetic energy, high Curie temperature, excellent thermal stability, and corrosion resistance [1]. They are currently used in magnetic couplings, motors, and actuators in automobiles and other vehicles [2,3]. The manufacturing process of samarium-cobalt magnets generates a large amount of scrap due to cutting. From another perspective, samarium is mixed with other rare earth and actinide elements in natural ores [4]. The separation of samarium from other rare earth elements and radioactive actinide elements requires time-consuming procedures while ensuring safety. Therefore, there is an industrial demand to recycle certain rare earth elements from scrap rather than obtaining the necessary rare earth elements from natural ores [5].

Rare earths are used in a variety of functional materials, but their supply is fraught with difficulties [6,7]. Specifically, rare earth ores can only be mined in certain areas of the world and usually contain radioactive elements [8]. Because mining of rare earths poses environmental problems, recycling rare earths from scrap and magnet waste may be a suitable alternative [9]. Based on these situations, several rare-earth recycling processes have been reported. For example, solvent extraction using dilute ionic liquids has been used to remove transition metals from mixtures with rare earth elements [10,11]. However, this process requires high concentrations of acid and special reagents. Alternatively, the chemical vapor transport could recover samarium from samarium-cobalt magnetic alloy sludge [12,13]. However, this method requires high temperatures and specialized equipment. The drawbacks of these processes call for the development of new technologies to improve current recycling methods.

Rare earth phosphates, the main component of rare earth ores, are known to be such stable compounds that they can exist stably in nature [14]. The method of refining rare earth elements from ores has been established and put into practical use. However, there are few reports on processes to recover rare earth elements as phosphates. The precipitation method is one of the most useful techniques for separating target metals from aqueous solutions in which other metals are mixed [15,16]. The precipitation method using inorganic reagents is particularly advantageous in that it does not use harmful organic solvents. Furthermore, the wastewater generated in this process is relatively easy to dispose of. In addition, the precipitation process can be easily estimated by using laboratory simulated solutions. Metal hydroxides are often used in precipitation techniques because they can efficiently recover large amounts of target metal compounds [17,18]. However, metal hydroxides lack the selectivity to form precipitations in the presence of precipitating agents. Therefore, a precipitation method to recover samarium from transition metal mixtures as phosphate

Eur. Chem. Bull. **2022**,11(8), 47 – 52

47

was recently reported [19].

In this study, we dissolve practical samarium magnets in various acids and attempt to recover samarium as phosphate using a precipitation method. Samarium magnets were dissolved using various concentrations of nitric acid, hydrochloric acid, and sulfuric acid to obtain samarium phosphate by a two-step precipitation method. This method allows us to obtain rare earth phosphates, the main component of rare earth ores, without the use of high temperatures or special equipment. Cobalt, iron, and copper hydroxides were precipitated and removed in step I. In step II, samarium phosphate was precipitated by adding phosphoric acid and adjusting the pH with sodium hydroxide.

MATERIALS AND METHODS

Materials: Samarium magnets were obtained from Magfine Corporation (Sendai, Japan). Other chemicals were commercially pure (FUJIFILM Wako Pure Chemicals Corporation, Osaka, Japan) and used without further purification.

Procedures: The flow of the experimental process is shown in Figure 1. First, the magnets were heated at 900 ºC for 1 hour to remove the magnetic force. To dissolve the demagnetized alloys (2.1 g), a 200 mL acid solution was prepared with chemically equivalent amounts of nitric acid, hydrochloric acid, and sulfuric acid. The composition of the magnet differs depending on the company, however in this study, it was calculated based on the composition described in previous paper [19]. As the results of the calculation, 4.5, 6.0 and 2.0 mL of nitric acid, hydrochloric acid and sulfuric acid were used respectively. In addition, the solutions using double and triple volumes of these acids were also prepared. The demagnetized alloys were placed in these acid solutions for 7 days. These solutions were filtered to remove the undissolved residue. Then, these solutions were adjusted to pH 4 using concentrated sodium hydroxide solution (step I). The formed precipitate was filtered and designated as "Precipitate I". To the filtered solutions, 1.0 mol/L phosphoric acid was added so that P/Sm=1/1. The amount of samarium in the magnet was calculated according to the composition described in the previous papers mentioned above [19]. These filtered solutions were then adjusted to pH 7 using concentrated sodium hydroxide solution (step II). The formed precipitate was filtered as Precipitate II. A part of the precipitates I and II was heated at 700ºC for 1 hour and subjected to X-ray diffraction (XRD) analysis.
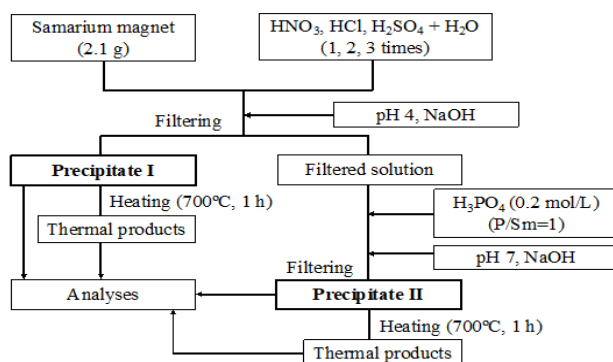

Figure 1. Experimental procedure.

Analytical methods: The crystalline phase compositions of the precipitates and their thermal products were analyzed by X-ray diffraction (XRD; MiniFlex, Rigaku Corp., Akishima, Japan) using monochromated Cu Kα radiation (30 kV, 15 mA, 3º/min). Infrared (IR) spectra were measured on a Horiba FT-IR 720 spectrometer (Horiba Ltd., Kyoto, Japan) using the KBr disk method (Resolution: 4 cm^{-1}, 16 times scanned). To estimate the ratios of samarium, cobalt, iron, and copper in the precipitates, a portion of the sample was dissolved in a nitric acid solution. These ratios were calculated from the results with Agilent 4200 Microwave Plasma Atomic Emission Spectroscopy (MP-AES). The color of the precipitates was estimated from the ultraviolet–visible (UV–Vis) reflectance spectra (UV2100; Shimadzu Corp., Kyoto, Japan) (reference compound: BaSO$_4$). The color of the materials was also estimated using a TES135 plus color analyzer (TES Electrical Electronic Corp, Taipei, Taiwan). The L* value represents the whiteness of the material, with 100 corresponding to white and 0 to black. The a* value represents the redness of the material, with positive values corresponding to red and negative values to green [20]. The b* value indicates the intensity of yellowness, with positive values corresponding to yellow and negative values to blue.

RESULTS AND DISCUSSION

Dissolution and Precipitate I

Table 1 shows the residual weight and ratio of magnet dissolved in various acids. Under the conditions in which more than twice as much nitric acid and three times as much hydrochloric acid were used, the magnet was almost dissolved. On the other hand, under the conditions where sulfuric acid was used, approximately 20% of the alloy remained undissolved regardless of the amount used.

Table 1 Residual weight and ratio of magnet

Acid	Amount of acid	Residual weight /g	Residual ratio /%
HNO$_3$	1	0.827	39.38
HNO$_3$	2	0.022	1.04
HNO$_3$	3	0.029	1.37
HCl	1	1.126	53.64
HCl	2	0.700	33.33
HCl	3	0.165	7.86
H$_2$SO$_4$	1	0.420	20.00

Eur. Chem. Bull. **2022**,*11*(8), 47 – 52

48

H$_2$SO$_4$	2	0.426	20.28
H$_2$SO$_4$	3	0.428	20.36

Since the precipitates I were formed in an aqueous solution, they tended to be amorphous [21]. In fact, precipitate I prepared with equivalent and doubled amounts of acid was amorphous when not heated. In the XRD pattern of the sample prepared with triple acid, the peaks of iron oxide and samarium oxide were observed. Samples were heated to crystallize the compounds contained in Precipitates I. Figure 2 shows XRD patterns of precipitates I prepared with various acids (1 time) and then heated at 700ºC. From these XRD patterns, it was confirmed that all samples contained Fe$_2$O$_3$. The peak of Sm$_2$O$_3$ was strongly observed in the condition using H$_2$SO$_4$. The purpose of Step I was to remove Co, Fe, and Cu compounds, and samarium ions had to remain in solution. Therefore, the condition using HNO$_3$ was considered to be suitable for the purpose of this study because there is no peak of samarium compound.
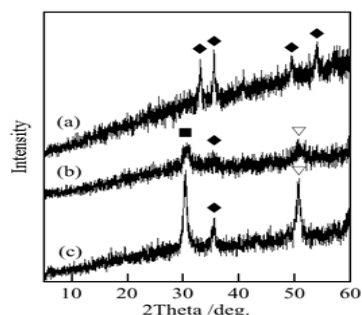

Figure 2. XRD patterns of precipitates I prepared with various acids (1 time) and then heated at 700ºC, (a) HNO$_3$, (b) HCl, (c) H$_2$SO$_4$, ∇; Sm$_2$O$_3$, ◆; Fe$_2$O$_3$, ■; Co$_3$O$_4$.

The colors of samarium, cobalt, iron, and copper compounds assumed in this study are pale yellow, pink, brown, and light blue, respectively. Of these, brown appears the strongest. Figure 3 shows the photographs of precipitates I prepared with various acids. Overall, precipitates I were brown powders. Samples using nitric acid became darker brown as the amount of acid increased. Conversely, sample using sulfuric acid became weaker brown color as the amount of acid increased. Table 2 shows the yields and L*a*b* results of precipitate I prepared with various acids. Under the condition using twice the amount of sulfuric acid, the amount of precipitate I was too small to analyze. When compared with the same amount of acid, a large amount of precipitate I was obtained when nitric acid was used.

Samples using nitric acid showed lower L* values and higher a* values than those using hydrochloric acid and sulfuric acid. These were considered to be due to the influence of iron compounds.
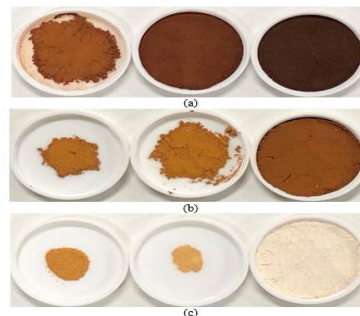

Figure 3. Photographs of precipitates I prepared with various acids, from left, 1, 2, 3 times of acid quantity, (a) HNO$_3$, (b) HCl, (c) H$_2$SO$_4$.

Table 2. Yields and L*a*b* results of precipitate I prepared with various acids

Acid	Amount of acid*	Yield /g	L*	a*	b*
HNO$_3$	1	0.303	44.22	23.66	30.47
HNO$_3$	2	0.907	35.74	20.95	20.54
HNO$_3$	3	0.965	32.97	17.60	15.58
HCl	1	0.092	62.04	10.12	24.88
HCl	2	0.187	61.29	10.34	29.82
HCl	3	0.779	46.69	16.37	26.98
H$_2$SO$_4$	1	0.111	68.70	6.01	22.37
H$_2$SO$_4$	2	0.010	-	-	-
H$_2$SO$_4$	3	0.318	88.20	4.26	9 .86

*; times of stoichiometric quantity

Table 3 shows MP-AES results of precipitate I prepared with various acids and recovery ratio of samarium. The samarium recovery ratios are for reference only, since the amount of samarium originally contained in the magnet is not known precisely [19]. The change due to the amount of acid was smaller than the change due to the type of acid. The Co/Sm, Fe/Sm, and Cu/Sm ratios were higher in the samples with nitric acid, which is due to the lower amount of samarium in precipitate I. The Fe/Sm ratios were particularly high, which was related to the tendency of iron compounds to precipitate in step I. Summarizing the above results, it was found that the use of nitric acid is most suitable for the purpose of step I.

Table 3 MP-AES results of precipitate I prepared with various acids and recovery ratio of samarium

Acid	Amount of acid*	Co/Sm	Fe/Sm	Cu/Sm	(Co+Fe+Cu)/Sm	Recovery of Sm /%
HNO$_3$	1	2.125	39.621	3.410	45.155	0.68
HNO$_3$	2	3.696	38.916	3.641	46.253	2.60
HNO$_3$	3	2.450	37.535	5.642	45.628	2.45
HCl	1	1.318	17.384	0.054	18.755	0.26
HCl	2	1.319	10.427	0.000	11.746	0.74
HCl	3	1.886	18.869	0.695	21.449	2.87
H$_2$SO$_4$	1	2.534	3.245	0.000	5.779	0.61
H$_2$SO$_4$	2	-	-	-	-	
H$_2$SO$_4$	3	0.145	0.078	0.000	0.223	17.43

*; times of stoichiometric quantity

Precipitate II

Precipitate II showed weak XRD peaks without heating, however was heated to make the XRD peak pattern clearer. Figure 4 shows XRD patterns of precipitates II prepared with various acids (1 time) and then heated at 700ºC. All samples showed a peak pattern of samarium phosphate. Figure 5 shows IR spectra of precipitates II prepared with various acids (1 time). The peak at 1630 cm^{-1} is attributed to water, and the peaks at 540, 620, and 1060 cm^{-1} are due to phosphate ion. Sample prepared with nitric acid had the peak at 1385 cm^{-1}, which is due to nitrate ion. It was confirmed that phosphoric acid added in step II was used for the formation of phosphate.
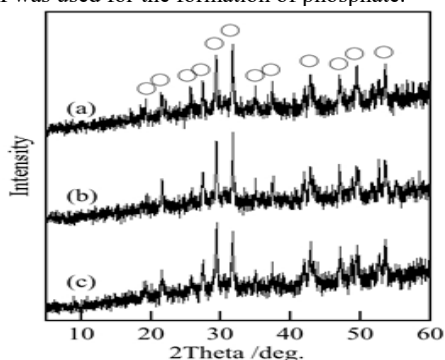

Figure 4. XRD patterns of precipitates II prepared with various acids (1 time) and then heated at 700ºC, (a) HNO₃, (b) HCl, (c) H₂SO₄, ○; SmPO₄.
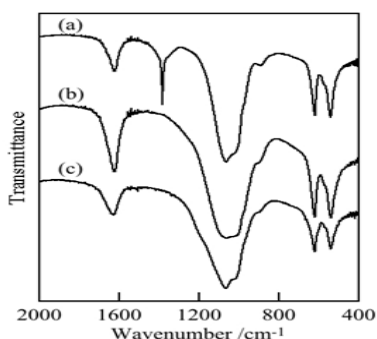

Figure. 5 IR spectra of precipitates II prepared with various acids (1 time), (a) HNO₃, (b) HCl, (c) H₂SO₄.

Figure 6 shows the photographs of precipitates II prepared with various acids. Since iron compounds were removed in step I, precipitates II became a light-colored powder as a whole. The light pink color suggested that samples contained cobalt compounds. Table 4 shows yields and L*a*b* results of precipitate II prepared with various acids. The change in the yield of precipitates II depending on the type and amount of acid was smaller than the change of precipitate I. All samples showed higher L* values than 84 and positive a* values, corresponding to whitish and weak reddish powders.
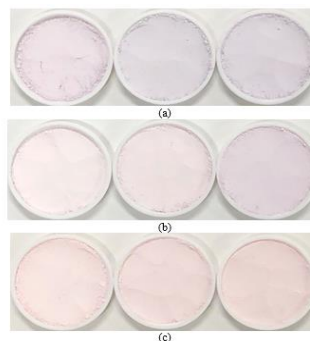

Figure 6. Photographs of precipitates II prepared under various conditions, from left, 1, 2, 3 times of acid quantity, (a) HNO₃, (b) HCl, (c) H₂SO₄.

Table 4. Yields and L*a*b* results of precipitate II prepared with various acids

Acid	Amount of acid*	Yield /g	L*	a*	b*
HNO₃	1	0.710	87.39	3.46	-0.15
HNO₃	2	1.100	88.17	1.57	1.65
HNO₃	3	1.142	84.59	1.96	1.82
HCl	1	0.672	90.90	3.77	1.84
HCl	2	0.983	92.46	4.51	0.53
HCl	3	1.215	89.96	4.36	-0.43
H₂SO₄	1	1.181	92.39	4.62	1.56
H₂SO₄	2	1.481	88.36	5.44	2.01
H₂SO₄	3	1.269	91.88	5.75	2.24

*; times of stoichiometric quantity

Figure 7 shows UV-Vis. reflectance spectra of precipitates II prepared with various acids. The peaks at 400 nm were due to samarium and the broad drops at 530 nm were due to cobalt compounds. The reflectance of the sample using nitric acid was slightly lower than the other samples. Since the cobalt, iron, and copper compounds clearly have absorption in the visible light region, the high reflectance of the samples indicates a high proportion of samarium compounds.
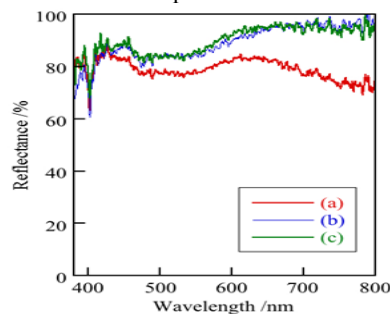

Figure 7. UV-Vis. reflectance spectra of precipitates II prepared with various acids (1 time), (a) HNO₃, (b) HCl, (c) H₂SO₄.

Table 5 shows MP-AES results of precipitate II prepared with various acids and recovery ratio of samarium. Samples prepared with nitric acid show a lower proportion of iron compounds, while those prepared with hydrochloric acid and sulfuric acid show a lower proportion of copper compounds. The effect of the amount of acid on the ratio of cations was small. Finally, the

(Co+Fe+Cu)/Sm ratio in samples was less than 0.5, and samarium phosphate could be selectively obtained.

Table 5. MP-AES results of precipitate II prepared with various acids and recovery ratio of samarium

Acid	Amount of acid*	Co/Sm	Fe/Sm	Cu/Sm	(Co+Fe+Cu)/Sm	Recovery of Sm /%
HNO$_3$	1	0.169	0.009	0.096	0.274	54.30
HNO$_3$	2	0.150	0.007	0.184	0.341	73.75
HNO$_3$	3	0.145	0.006	0.161	0.313	80.59
HCl	1	0.075	0.069	0.000	0.144	52.01
HCl	2	0.093	0.069	0.000	0.162	67.47
HCl	3	0.145	0.097	0.005	0.247	71.39
H$_2$SO$_4$	1	0.132	0.095	0.000	0.227	56.72
H$_2$SO$_4$	2	0.038	0.056	0.000	0.094	85.86
H$_2$SO$_4$	3	0.118	0.095	0.000	0.213	67.88

*; times of stoichiometric quantity

Table 6. Residual ratios of each cation in filtered solution

Acid	Amount of acid	Sm /%	Co /%	Fe /%	Cu /%
HNO$_3$	1	0.00	65.90	0.00	12.67
HNO$_3$	2	0.00	92.04	0.00	36.31
HNO$_3$	3	0.00	83.45	0.00	27.51
HCl	1	0.05	41.98	1.44	37.69
HCl	2	0.00	94.31	1.25	0.00
HCl	3	0.00	72.47	1.30	30.20
H$_2$SO$_4$	1	0.01	83.76	40.05	0.00
H$_2$SO$_4$	2	0.01	75.84	35.58	0.00
H$_2$SO$_4$	3	0.02	69.22	33.07	0.00

Table 6 shows the percentage of each cation remaining in the filtrate. After the recovery of precipitate II, it was observed that almost no samarium cations remained. When nitric acid and hydrochloric acid were used, cobalt and copper cations were confirmed to remain, and when sulfuric acid was used, cobalt and iron cations were confirmed to remain.

CONCLUSION

In this study, samarium phosphate was obtained from practical magnets by a two-step precipitation method. Using twice the amount of nitric acid and three times the amount of hydrochloric acid, most of the magnets could be dissolved. The use of nitric acid allowed the most selective precipitation removal of compounds other than samarium, and the final precipitate II was found to have a sufficiently low (Co+Fe+Cu)/Sm ratio.

Conflict of interest: None.

REFERENCES

i.   Akhtar S., Khan A. N., Khan M., Jaffery S. H. I., Effect of solidification process on the magnetic properties of samarium cobalt intermetallic compounds, Materials Transactions, 2020, 61(5), 1008-1013.https://10.2320/matertrans.MT-M2019269

ii. [2] Nordelof A., Grunditz E., Lundmark S., Tillman A. M., Alatalo M., Thiringer T., Life cycle assessment of permanent magnet electric traction motors, Transportation Research D, 2019, 67, 263-274. https://doi.org/10.1016/j.trd.2018.11.004

iii. [3] Zhou X., Huang A., Cui B., Sutherland J. W., Techno-economic assessment of a novel SmCo permanent magnet manufacturing method, Procedia CIRP, 2021, 98, 127-132. https://10.1016/j.procir.2021.01.017

iv. [4] Kumari A., Jha S., Patel J. N., Charkravarty S., Jha M. K., Pathak D. D., Processing of monazite leach liquor for the recovery of light rare earth metals (LREMs), Minerals Engineering, 2018, 129, 9-14. https://doi.org/10.1016/j.mineng.2018.09.008

v.   [5] Jyothi R.K., Thenepalli T., Ahn J. W., Parhi P. K., Chung K. W., Lee J., Review of rare earth elements recovery from secondary resources for clean energy technologies: Grand opportunities to create wealth from waste, Journal of Cleaner Production, 2020, 267, 122048. https://doi.org/10.1016/j.jclepro.2020.122048

vi. [6] Li W., Xiong C. Y., Jia L. C., Pu J., Chi B., Chen X., Schwank J. W., Li J., Strontium-doped samarium manganite as cathode materials for oxygen reduction reaction in solid oxide fuel cells, J. Power Sources, 2015, 284(15), 272-278. https://doi.org/10.1016/j.jpowsour.2015.03.027

vii. [7] Danchova N., Gutzov S., Time evolution of samarium doped silica sol–gel materials followed by optical spectroscopy, J. Sol-Del Sci. Technol., 2013, 66, 248-252. https://doi.org/10.1007/s10971-013-3001-1

viii.[8] Demol J., Ho E., Senanayake G., Sulfuric acid baking and leaching of rare earth elements, thorium and phosphate from a monazite concentrate: effect of bake temperature from 200 to 800ºC, Hydrometallurgy, 2018, 179, 254-267. https://doi.org/10.1016/j.hydromet.2018.06.002

ix. [9] Hengkai L., Feng X., Qin L., Remote sensing monitoring of land damage and restoration in rare earth mining area in 6 countries in southern Jiangxi Based on multisource sequential images, Journal of Environmental Management, 2020, 267, 110653. https://doi.org/10.1016/j.jenvman.2020.110653

x. [10] Hoogerstraete T. V., Binnemans K., Highly efficient separation of rare earths from nickel and cobalt by solvent extraction with the ionic liquid trihexyl(tetradecyl)phosphonium nitrate: a process relevant to the recycling of rare earths from permanent magnets and nickel metal hydride batteries, Green Chem., 2014, 16, 1594-1606. https://doi.org/10.1039/c3gc41577e

xi. [11] Hoogerstraete T. V., Wellens S., Verachtert K., Binnemans K., Removal of transition metals from rare earths by solvent extraction with an undiluted phosphonium ionic liquid: separations relevant to rare-earth magnet recycling, Green Chem., 2013, 15, 919-927. https://doi.org/10.1039/C3GC40198G

xii. [12] Li K., Chen J., Zou D., Liu T., Li D., Kinetics of nitric acid leaching of cerium from oxidation roasted Baotou mixed rare earth concentrate, Journal of Rare Earth, 2019, 37(2), 198-204. https://doi.org/10.1016/j.jre.2018.05.015

xiii. [13] Stinn C., Allanore A., Selective sulfidation for rare earth element separation, Rare Metal Technology 2022, 2022, 259-278. https://doi.org/10.1007/978-3-030-92662-5_25

xiv. [14] Lazo D. E., Dyer L. G., Alorro R. D., Browner R., Observations of the varied reactivity of xenotime and monazite in multiple systems, Minerals Engineering, 2020, 159, 106633. https://doi.org/10.1016/j.mineng.2020.106633

xv. [15] Chen J., Zhang H., Zeng Z., Gao Y., Liu C., Sun X., Separation of lithium and transition metals from the leachate of spent lithium-ion battery by extraction-precipitation with p-tert-butylphenoxy acetic acid, Hydrometallurgy, 2021, 206, 105768. https://doi.org/10.1016/j.hydromet.2021.105768

xvi. [16] Cai Y., Ma L., Xi X., Nie Z., Nie Z., Separation of tungsten and molybdenum using selective precipitation with manganese sulfate assisted by cetyltrimethil ammonium bromide (CTAB), Hydrometallugy, 2020, 198, 105494. https://doi.org/10.1016/j.hydromet.2020.105494

xvii. [17] Hunang J., Huang Z. L., Zhou J. X., Li C. Z., Yang Z. H., Ruan M., Li H., Zhang X., Wu Z. J., Qin X. L., Hu J. H., Zhou K., Enhancement of heavy metals removal by microbial flocculant produced by Paenibacillus polymyxa combined with an insufficient hydroxide precipitation, Chemical Engineering Journal, 2019, 374, 880-894. https://doi.org/10.1016/j.cej.2019.06.009

xviii. [18] Pohl A., Removal of heavy metal ions from water and wastewaters by sulfur-containing precipitation agents, Water, Air, and Soil Pollution, 2020, 231, 503. https://doi.org/10.1007/s11270-020-04863-w

xix. [19] Onoda H., Kurioka Y., Selective removal and recovery of samarium from mixed transition metal solution using phosphoric acid, J. Environ. Chem. Eng., 2016, 4(4), 4536-4539. https://doi.org/10.1016/j.jece.2016.10.018

xx. [20] Kumari L. S., Rao P. P., Radhakrishnan A. N. P., James V., Sameera S., Koshy P., Brilliant yellow color and enhanced NIR reflectance of monoclinic $BiVO_4$ through distortion in VO_4^{3-} tetrahedral, Sol. Energy Mater. Sol. Cells, 2013, 112, 134-143. https://doi.org/10.1016/j.solmat.2013.01.022

xxi. [21] Yang G., Guo Q., Yang D., Peng P., Li J., Disperse ultrafine amorphous SiO_2 nanoparticles synthesized via precipitation and calcination, Coll. Surf. A, 2019, 568, 445-454. https://doi.org/10.1016/j.colsurfa.2019.02.041

Eur. Chem. Bull. **2022,**11(8), 47 – 52

52